Scanning Microscopy

Volume 4 | Number 2 Article 20

4-9-1990

Techniques for the Microanalysis of Higher Plants with Particular Reference to Silicon in Cryofixed Wheat Tissues

M. J. Hodson
School of Biological and Molecular Sciences

A. G. Sangster
York University

Scanning Microscopy, Vol. 4, No. 2, 1990 (Pages 407-418) 0891-7035/90$3.00+.00
Scanning Microscopy International, Chicago (AMF O'Hare), IL 60666 USA

TECHNIQUES FOR THE MICROANALYSIS OF HIGHER PLANTS WITH PARTICULAR REFERENCE TO SILICON IN CRYOFIXED WHEAT TISSUES

M.J. Hodson[1] and A.G. Sangster

Division of Natural Sciences, Glendon College, York University,
2275 Bayview Ave., Toronto, Ontario, M6N 3M6, Canada

[1] Present address: School of Biological and Molecular Sciences, Oxford Polytechnic, Gipsy Lane, Headington, Oxford, OX3 0BP, U.K., Telephone: (0865) 819240

(Received for publication December 10, 1989, and in revised form April 9, 1990)

Abstract

The applications of x-ray microanalysis in research into silicon in higher plants are reviewed, recent developments are assessed, and new data are presented. Conventionally prepared material [air or freeze drying for scanning electron microscopy (SEM), and glutaraldehyde/osmium tetroxide fixation for transmission electron microscopy (TEM)] has been studied using both wavelength and energy dispersive microanalysis. These techniques are reliable provided that the deposited form of silica is the major focus of investigation. Recently, studies concerning the soluble, mobile forms of silica, and the ionic environment at deposition sites have been initiated. In these investigations x-ray microanalysis has been carried out on the cold stage of an SEM, or after freeze substitution on sections in TEM. Two other developments which are considered are the use of proton induced x-ray emission, and electron energy loss spectroscopy.

To illustrate the most recent developments in this field we present new observations on mineral distribution in the culm and awn of wheat using microanalysis of frozen hydrated material in SEM, and in the wheat leaf using freeze substitution and TEM and scanning transmission electron microscopy.

Key Words: X-ray Microanalysis, Cryotechniques, Freeze Substitution, Silicon, Calcium, Wheat, Culm, Awn

*Address for Correspondence:
A.G. Sangster,
Division of Natural Sciences,
Glendon College, York University,
2275 Bayview Ave.,
Toronto, Ontario, M6N 3M6, Canada
Telephone: (416) 487-6732

Introduction

In higher plants silicon is taken up from the soil, is transported through the plant in soluble form, and is mostly deposited as amorphous silica in cell walls and lumina. Once deposited the amorphous silica is inert and not available for retransport. The microanalyst interested in silica in higher plants is presented with two problems: the analysis of the deposited form, and the analysis of the soluble form(s). The first of these problems has received much attention, but the second has only recently been tackled.

Recent reviews of silica deposition in higher plants include those on the shoots (Kaufman et al., 1981), the roots (Sangster and Parry, 1981), silicon physiology (Raven, 1983), and also the metabolic, health and ecological aspects (Werner and Roth, 1983; Parry et al., 1984; Sangster and Hodson, 1986).

Technical advances in silicon detection have been reviewed previously (Sangster and Parry, 1981; Sangster and Hodson, 1986). The only review to focus on the use of microanalysis in plant silica studies is that by Harvey (1986), which was restricted, since other applications of microanalysis were included. We shall describe the newer microanalytical techniques for the analysis of silicon in plant tissues, and also new data obtained from applications of cryotechniques.

Electron-probe X-ray Microanalysis and Scanning Electron Microscopy of Conventionally Prepared Material

Lauchli and Schwander (1966) first detected silicon in a higher plant organ (maize leaf) using this technique. This was followed by other studies including Laroche (1967) and Kaufman et al. (1969). In these investigations, wavelength dispersive analysis was used on conventionally prepared material (air drying or freeze drying). Silica deposits are ideal subjects for this kind of approach, as they are very stable in the electron beam, and elemental loss and redistribution is minimal. However, the advent of energy dispersive x-ray microanalysis (EDX) in the 1970s, permitted simultaneous analyses for all elements with the atomic number 11 (of Na) and above. Initially most work was carried out using scanning electron microscopy (SEM) in combination with EDX; examples of early studies include: Dayanandan and Kaufman (1976) working on the trichomes of Cannabis sativa; Dayanandan et al. (1976) who investigated the grass pulvinus; and Hansen et al. (1976) who

studied silica deposition in the salt marsh grass Distichlis spicata.

Gartner et al. (1984) analysed microdrops (less than 1 nl) of the xylem exudate of wheat roots using a wavelength dispersive electron probe. They measured soluble silicon quantitatively finding up to 10 mM in xylem exudate.

More recent examples of work using SEM and EDX include the investigation of silica deposition in the inflorescence bracts of Phalaris canariensis (Perry et al., 1984a) and wheat (Hodson and Sangster, 1989b). Since conventional preparation of the plant material is employed, these microanalyses are adequate provided that the silica deposits are the major focus of study. When the soluble ions associated with the deposits or the soluble pre-deposition forms of silicon are of interest then some type of cryotechnique is usually preferable.

TEM and EDX in conventionally prepared material

Transmission electron microscopy (TEM) was first used to study sections of silica deposits in the early 1970s (e.g., Kaufman et al., 1970). Generally, the preparatory techniques used were conventional glutaraldehyde and/or osmium tetroxide fixation, followed by embedding in resin, and sectioning onto water, usually with a diamond knife. As wavelength and EDX detectors became available, they were soon being fitted onto transmission electron microscopes, and were used to investigate silica deposits beginning in the mid 70s. Silica deposits are electron opaque, but can be confused with other types of deposited material in plant tissues. Microanalysis confirms that a deposit is siliceous. Most detectors used have been of the EDX type, the one exception being an early study of silica deposition in the root of Sorghum bicolor using wavelength dispersive analysis by Sangster and Parry (1976). Early investigations using TEM and EDX were those of Parry and Kelso (1977) on the roots of Saccharum officinarum, and Montgomery and Parry (1979) on the deposits found in the intercellular spaces of the roots of Molinea caerulea. Root studies were followed by those of Dinsdale et al. (1979) on the leaf mesophyll cell walls of Lolium multiflorum, and that of Sakai and Thom (1979) on the stomatal apparatus of sugar cane. The technique was also used by Heath (1981) to investigate silicon deposition in cowpea cells as a response to infection by an incompatible isolate of the cowpea rust fungus.

We have used conventional preparation, TEM and EDX to study the development of silica deposition in the lemma and glume of Phalaris canariensis (Hodson et al., 1984, 1985). This methodology allows for greater spatial resolution than SEM, and while satisfactory for immobile deposited forms of silicon, it is, however, inadequate for investigations concerning the transport pathways of soluble silicon and the ionic environment at deposition sites. It has often been observed that soluble components are leached from, or redistributed within, tissues during conventional preparation. The radioisotope of silicon, 31Si, has a half-life of only 156 minutes, which makes it unsuitable for most higher plant investigations. However, Mehard and Vocani (1975) were able to use this isotope to label diatoms. They found that 25-30% of ^{31}Si was lost from these organisms during conventional preparation, with most loss occurring during glutaraldehyde fixation. Thus, soluble silicon remaining in the organisms will have been redistributed. We assume that loss and redistribution of soluble silicon will occur similarly in higher plant tissues.

One possible method of preventing this is to freeze-dry plant material, and then infiltrate and embed it in resin. Eschrich et al. (1988) used this technique to assess mineral partitioning in the senescing leaves of beech. Using EDX they showed that Mg, K and P were retrieved from the leaf prior to shedding, S and Ca remained in the leaf, and Si and Cl accumulated in the leaf before shedding. The technique of freeze-drying followed by resin infiltration has been criticized on the grounds that it is too rapid a procedure, and that the vacuolar ions must undergo some redistribution when water is removed. Recently, Fritz (1989) demonstrated that reliable ion localization can be obtained in freeze-dried resin-embedded plant tissue, even in vacuoles. However, most investigators interested in diffusible ion localization have chosen cryo-SEM or freeze substitution and TEM. Our investigation of the ultrastructure of wheat leaf silica bodies, which follows, employs freeze substitution.

Plant culture and preparation for analysis

Triticum aestivum L. cv. Wheaton was grown in nutrient solution for two weeks under controlled conditions (Hodson and Sangster, 1988a). Segments of the basal leaves were excised from mature 20 cm long blades, at 7-7.5 cm behind the tip, and were quench-frozen by quick immersion in stirred supercooled propane (-186°C). They were then substituted in ether followed by embedment in Spurr's resin (Hodson and Bell, 1986). Thin sections (90 nm) were cut onto water using an LKB III ultramicrotome fitted with a DuPont diamond knife. The sections were collected on Formvar coated copper grids, stained in aqueous uranyl acetate, and lead citrate (Reynolds, 1963), and were photographed in an AEI Corinth TEM operating at 60 kV. These stained sections were necessary for obtaining good micrographs (Fig. 1), since the thick dry sections cut for microanalysis produced poor images in TEM.

Epidermal silica deposits

In Fig. 1, an epidermal silica cell of the basal leaf is sectioned to show the lumen filled with hydrated amorphous silica. At this stage of leaf development, most silica deposits are confined to silica cells (idioblasts). Deposition occurs following protoplasmic degeneration (Kaufman et al., 1981), and forms discrete silica bodies or phytoliths which extend in rows above the veins. The lumen deposit is opaque and composed of small particles which have been interpreted as fracture fragments due to the extreme hardness of opaline silica (Sangster and Parry, 1981), and also as sub-units or rods, characteristic of the ultrastructure (Kaufman et al., 1970; Dayanandan, 1983). In Fig. 1, most of the deposit has fallen out of the section. Particles of the deposit can be seen adhering to the thin outer tangential wall (OTW), but have become separated from it in the upper right corner of the cell. The radial and inner tangential walls (ITW) are thickened, and the particles appear to be embedded slightly in these wall surfaces. A TEM study of the abaxial epidermis of the glume (inflorescence bract) of the grass Phalaris canariensis L. (Hodson et al., 1985) revealed a transectional ultrastructure of mature silica cells similar to that shown in Fig. 1.

As their outline in planar view resembles that

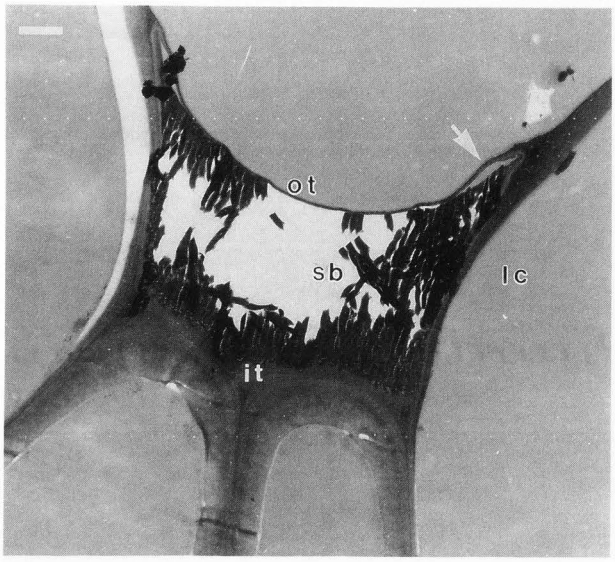

Figure 1. Transmission electron micrograph of a transverse section through a silica cell above the vein on the adaxial epidermis of the basal leaf blade of Triticum aestivum L. The lumen was completely infilled by opaque amorphous silica, including the gap, forming a solid silica body (sb), consisting of small particles. The silica body shattered during sectioning and a portion of the deposit has dropped out. Particles adhere to the thin outer tangential wall (ot) except in the upper right corner of the cell where the wall has separated from the particle bases (arrow). The radial walls and inner tangential wall (it) are considerably thicker, as are the walls of adjacent long cells (lc). Scale bar = 1 micrometer.

---

of the enclosing cell, the phytoliths of grasses and cereals (Gramineae) can be an important diagnostic tool in archaeological and palaeobotanical investigations. Phytoliths occur in soil as microfossils, and are classified according to their shapes and sizes (Metcalfe, 1960; Ollendorf, 1987; Hodson and Sangster, 1988b; Piperno, 1988).

SEM and EDX on a Cryostage

In the mid 70s the first publications appeared in which plant material was analysed by EDX on the cold stage of an SEM (for a review see Harvey, 1986). This technique should allow minimal redistribution of ions within the tissue, prior to analysis, enabling one to locate soluble silica; whereas in conventional preparation, soluble ions are removed, allowing only for detection of deposited silicon in walls. Using cryopreparation, we were able to locate soluble silica in plant tissues where previous conventional work had indicated none was present (Hodson and Bell, 1986; Hodson and Sangster, 1989c). The cryotechnique also allows for detection of other elements at silicification sites. Although the analytical resolution of several micrometers does not permit determination of spatial relationships, the presence of other elements such as K, Cl and Ca has been ascribed to involvement in the deposition mechanism (Perry et al., 1984a). This cannot be inferred from close localization alone; however, mono- and divalent cations are known experimentally to promote silica sol-gel transformations (Iler, 1955).

EDX identifies elemental silicon only, not indicating whether it is soluble or deposited (polymerized). In the following section, the distinction between "soluble silica" (e.g. monosilicic acid) and "deposited silica" (amorphous opal or silica gel) is made upon indirect criteria. Soluble silica is assumed to be the form present in many cell protoplasts because: (i) of the very low Si peaks generated, in contrast to deposited silica, defined as that characterized by consistently high Si peaks as well as by visible electron opacity in TEM; and (ii) the precise locations of silica deposits in lumens are known from previous studies of the wheat tissues (Hodson and Sangster, 1988a, 1988b).

Hodson and Sangster (1988a) investigated wheat leaves using cryo-SEM detecting Si, P, Cl, S, K and Ca. High Si levels were recorded in the epidermis, with lesser amounts in internal tissues. Ca was localized in the epidermis, higher levels being recorded in the adaxial epidermis.

The wheat root has also been studied using cryo-SEM and EDX, and the results were corroborated by repeating the study using freeze substitution and TEM (Hodson and Sangster, 1989c). Silica was deposited in the endodermal walls, and several other elements were detected at the deposition sites. Sorghum and other genera of the grass tribe Andropogoneae exhibit large silica deposits on the endodermal walls (Parry et al., 1984). Therefore, we used cryo-SEM to investigate ion localization in the roots of Sorghum bicolor (Hodson and Sangster, 1989a). Ca was detected in the silica aggregates, raising the question of its involvement in the deposition mechanism. The other elements detected were K, Cl, S, Na and P. To extend these studies, we used the cryo-SEM to investigate mineral distribution and biomineralization in the culm and lemma awn of wheat.

Mineral Distribution and Biomineralization in the Culm and Lemma Awn of Wheat

Plant culture, sampling and analysis

Triticum aestivum L. cv. Wheaton grains were germinated in a 4:2:2:1 mixture of topsoil, sand, vermiculite and peat moss in pots outside in full exposure to solar radiation in Toronto. After 8 weeks the plants began to flower. Harvesting codes are based upon the initial exsertion of the inflorescence spike (head) at the apex of the culm (stalk) into the atmosphere above the enclosing sheath of the uppermost (flag) leaf. At the initial emergence of the tips of the long awns borne by the lemma (inflorescence bract) a harvest was taken and was designated as EO. There were also two harvests at one and 14 days before emergence (E-1 and E-14), and one harvest seven days after emergence (E+7).

For microanalysis samples of the culm (0.5 cm in length) were cut from the region about 1.0 cm below the junction with the inflorescence. The length of the inflorescence at E-1 and E0 was 7-8.0 cm, while the internode at these harvests was enclosed by leaves, and located 8-9.0 cm below the emergence point. At E+7, spike length was 9.5 cm and the terminal culm internode was fully exposed.

Awns were removed from lemmas in the central region of the spike, and 1 cm long segments of the awns were excised from the middle region. At the

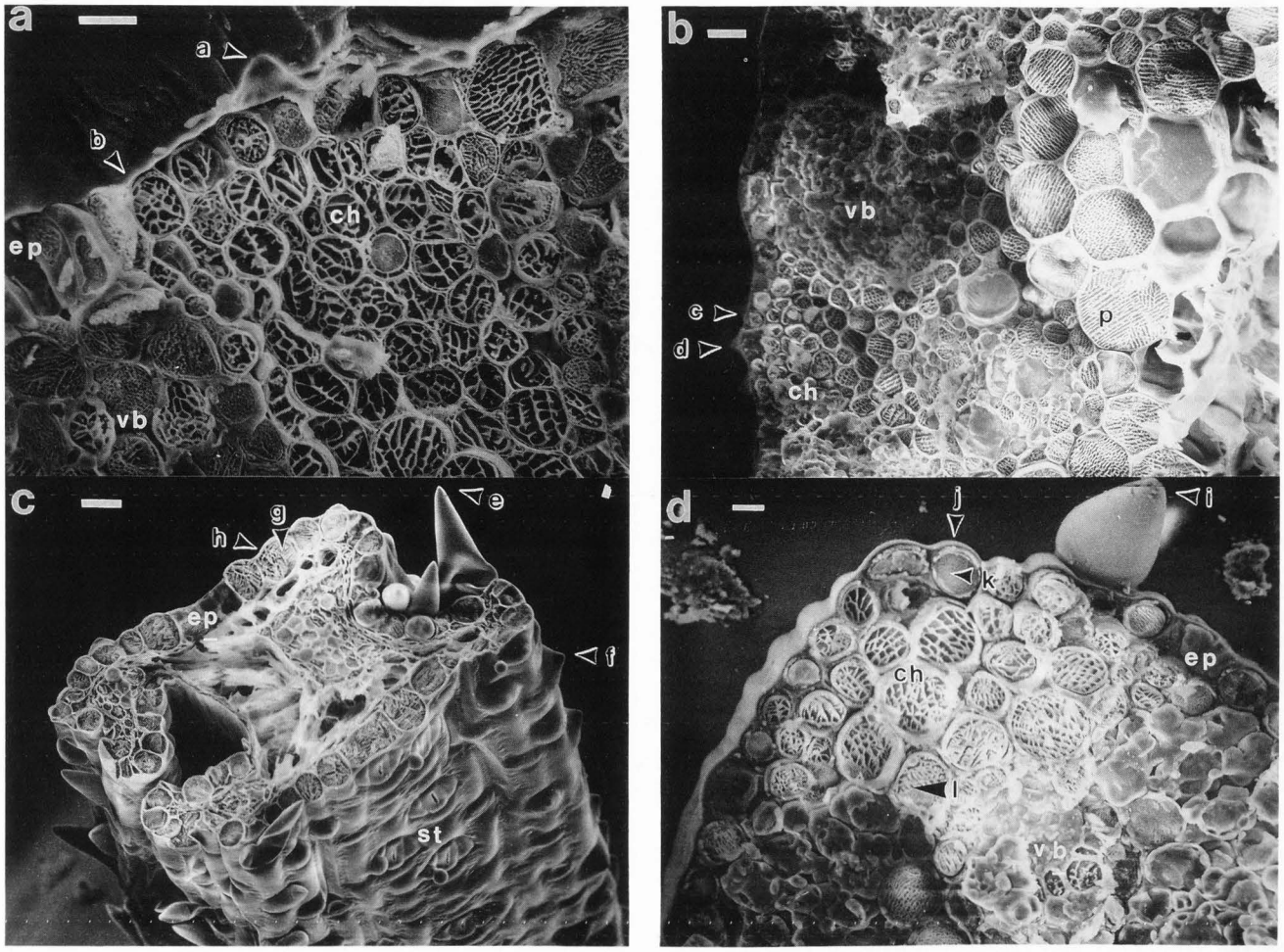

Figure 2. Scanning electron micrographs of transverse fractures of bulk-frozen tissues of T. aestivum. Each letter with arrow indicates a specific cell microanalysis point whose spectrum has the same letter in Fig. 3. **(a)** Culm internode, E-1 harvest. The outer region consists of peripheral vascular bundles (vb) alternating with bands of chlorenchyma (ch). Microanalysis points (a and b) are located on a papilla tip and the outer tangential wall (OTW) of a long cell of the epidermis (ep). Scale bar = 10 micrometers. **(b)** Culm internode, E+7, outer regions. The peripheral sclerenchyma encloses small vascular bundles (vb) alternating with chlorenchyma (ch). Larger vascular bundles surrounded by ground parenchyma (p) occur internally. Microanalysis points (c and d) are located on an epidermal long cell OTW and a papilla wall. Scale bar = 20 micrometers. **(c)** Awn of lemma, E-14, fractured at mid-length. Microanalysis points (e, f, g and h) located on prickle wall, papilla wall, the protoplasm and OTW of a long cell of the epidermis (ep). Stomatal rows (st) visible below fracture. Scale bar = 20 micrometers. **(d)** Awn of lemma, E+7, mid-length. Microanalysis points (i, j, k and l) located on prickle wall, OTW and protoplasm of long cell of the epidermis (ep), and on the protoplasm of an outer bundle sheath cell. Vascular bundle (vb), chlorenchyma (ch). Scale bar = 10 micrometers.

E-14 harvest, the awns were 4 cm long and were positioned 12 cm below exsertion, covered by three leaf layers. At E-1, the awns were 5 cm long and 2 cm below exsertion. The E+7 awns had been exposed for one week, and were 6 cm long.

Tissues were first plunged into supercooled liquid nitrogen under vacuum in an EM Scope SP 2000 cryosystem. These specimens were fractured transversely, etched at -90°C for 15 miniutes and coated with chromium. The material was then transferred to a SP 2000 system cold stage (-180°C) in an ISI DS130 SEM. Before analysis, specimens with uneven fracture surfaces were rejected. Analyses were obtained using a PGT System 4 energy dispersive microanalysis system operating at 15 kV, working distance of 25-30 mm, beam diameter of 300 nm, take-off angle of 26°, and a collection time of 40 sec (Hodson and Sangster, 1988a). Analytical results are shown as x-ray spectra with 0-5 keV horizontal scales, and variable vertical scales (vs) in counts.

Ion localization and silicification of immature stages of the culm

Figure 2a shows the outer region of the E-1 culm with analysis points on papilla and long cell walls, while the corresponding spectra are shown in Figs. 3a, b. These culms were not exposed. For E-1 and EO culms higher silicon peaks were recorded for the following tissues: the lumina of xylem vessels

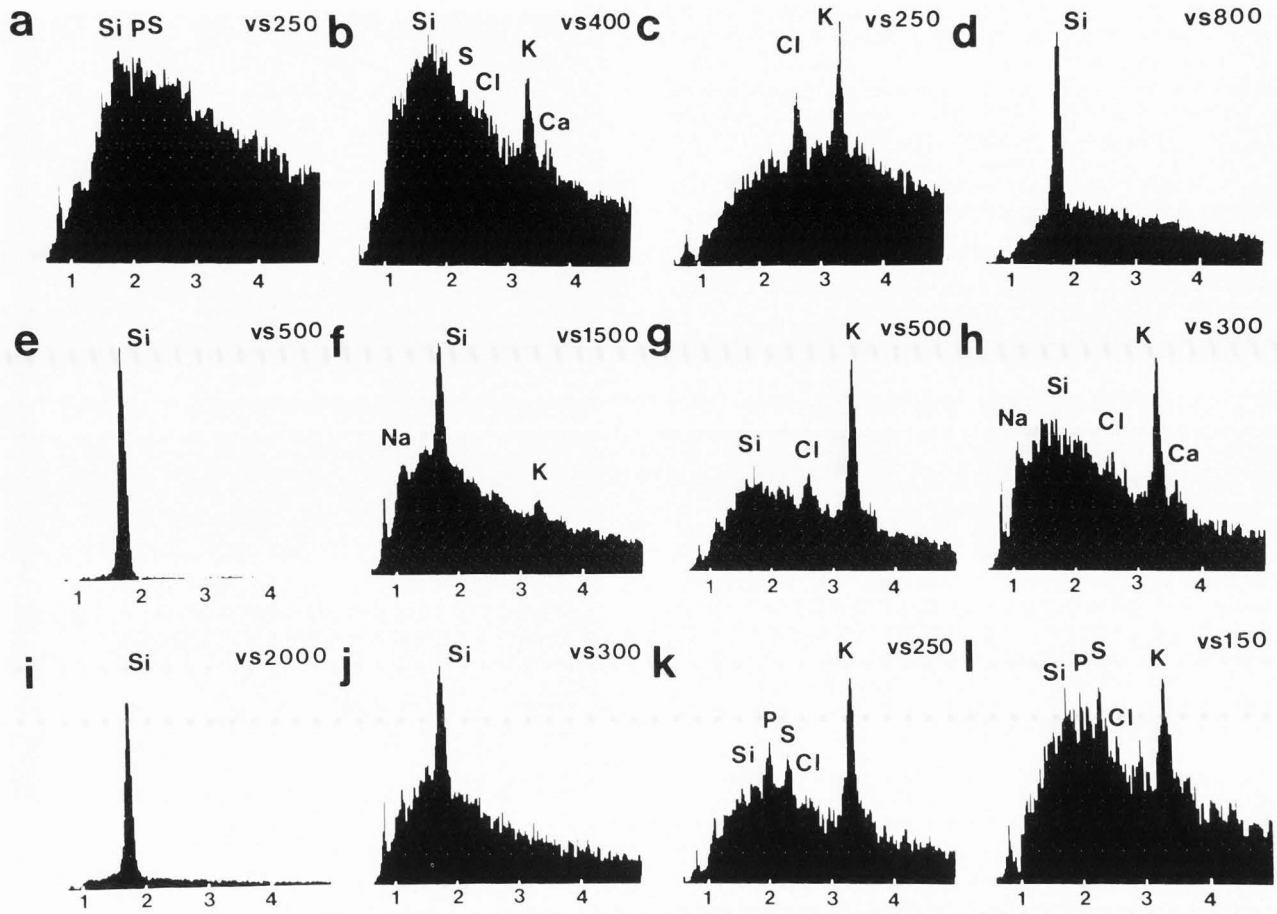

Figure 3. All diagrams are X-ray spectra from fracture surfaces of bulk-frozen culms and awns of wheat. Vertical scales (vs) are in counts. Horizontal scales are in keV. The corresponding microanalysis points for all spectra are shown in Fig. 2. Spectra, harvest and reference fracture surface micrographs are as follows: **a and b**: E-1 culm, see Fig. 2a; **c and d**: E+7 culm, see Fig. 2b; **e - h**: E-14 awn, see Fig. 2c; **i - l**: E+7 awn, see Fig. 2d. All microanalysis points are epidermal except for 1. The tissue locations for individual spectra are: **a**: tip of papilla wall; **b**: outer tangential wall (OTW) of long cell; **c**: OTW of long cell; **d**: tip of papilla wall; **e**: tip of prickle wall; **f**: tip of papilla wall; **g**: protoplasm of long cell; **h**: OTW of long cell; **i**: tip of prickle wall; j: OTW of long cell; **k**: protoplasm of long cell; and **l**: protoplasm of outer bundle sheath cell.

from the outer bundle circle, the parenchyma walls and protoplasts extending out to the epidermis, and the OTW of the epidermis. A similar pathway was previously postulated for the wheat leaf (Hodson and Sangster, 1988a). Small silicon peaks were detected in the walls of ground parenchyma bordering the central cavity of the EO culm. K was almost ubiquitous in distribution and the highest P levels were recorded in the xylem lumina, and epidermal protoplasts.

Figure 2b shows the outer region of the E+7 culm with epidermal analysis points indicated, and the corresponding spectra are shown in Fig. 3c, d. Silicon peaks for the epidermal walls and protoplasts are generally higher than for previous harvests (e.g., papillae: cf. Figs. 3d and 3a). The results for long cells are similar (not shown). In some cases the ITW of some long cells is not yet silicified (Fig. 3c). In contrast, subepidermal sclerenchyma and chlorenchyma exhibit small silicon peaks, with none present in parenchyma bordering the central cavity.

In the immature (non-emerged) culm (E-1), silicon is distributed throughout the tissues, but is beginning to localize preferentially in specific epidermal cells. After emergence (E+7), silicon levels increase in peripheral tissues, especially the epidermal OTW. By maturity, peripheral localization intensifies, as shown previously for mature culms of barley and maize (Hayward and Parry, 1973; Bennett and Sangster, 1982). Silicon in the epidermal OTW confers structural rigidity. Gartner and Paris-Pireyre (1984) detected more deposited silica in the culms of a wheat cultivar (Tarasque) which was resistant to lodging than in a susceptible cultivar (521). Rice cultivars which were resistant to stem boring insect larvae contained denser deposits of silica in the culm epidermis (Djamin and Pathak, 1967). Silica protects against insect and fungal attack in a number of crop plants (see review by Eleuterius and Lanning, 1987).

Ion localization and silicification of immature stages of the awn

Transverse fractures of the awn are shown in Figs. 2c (E-14) and 2d (E+7). Four spectra (Fig. 3e, f, g and h) accompany the corresponding epidermal

microanalysis points in Fig. 2c. Na, Si, P, S, Cl, K and Ca were detected in most E-14 awn tissues. High K peaks were detected in the epidermal protoplasts. At E-14 silicon is the dominant element in the prickle wall tip (Fig. 3e), and in the papilla (Fig. 3f), while it has only begun to accumulate in the long cell protoplasm and OTW (Fig. 3g, h). The small whitish (etiolated) awns are attached to a juvenile inflorescence spike which was unexposed and covered by leaf sheaths. In contrast, the E+7 awns at the flowering stage are green. Microanalysis points for the E+7 harvest (Fig. 2d) exhibit silicon peaks for the epidermal prickles (Fig. 3i) and papillae (not shown) similar to those at E-14. However, the long cell OTW shows a massive increase in silicon (cf. Fig. 3j and h). Silicon levels are low in protoplasts of the epidermis (Fig. 3k) and outer bundle sheath cells (Fig. 3l). The former consistently show high K peaks.

Similar results were obtained for the EO awns (data not shown), except that high silicon levels additionally occur in the OTW of some long cells. Low levels of silicon and Ca were detected variously in walls and protoplasts of all internal chlorenchyma, vascular and ground tissues. Generally, 3 to 7 analyses were obtained for each cell type, and representative spectra are shown in Fig. 3. Silica deposits normally exhibit considerable deviation, but other elements (e.g. Ca) show very much less. This comparison is also valid for Table 1.

The occurrence of relatively high silicon levels in the walls of epidermal prickles and papillae of juvenile (E-14) awns (Fig. 3e, f) is unexpected. This significant finding challenges the passive model which accounts for all silica deposition in the shoot on the basis of evapotranspiration (see Kaufman et al., 1981 for a critique). This concept is obviously flawed as a mechanism accounting for biomineralization in such juvenile tissues. Previously, initial silicification of prickles and papillae of the glume (inflorescence bract) of the grass Phalaris canariensis L. was found to occur one week before head emergence (Sangster et al., 1983; Hodson et al., 1985). These epidermal cells are also initial silicification sites in other graminaceous species (for reviews, see Kaufman et al., 1981; Sangster et al., 1983). In barley, silicification is initiated at the tip of the awn after emergence (Hayward and Parry, 1973), which contrasts with the E-14 results for wheat. Following the early developmental stages, silica becomes increasingly incorporated into all epidermal tissues of the mature awn (seed ripe stage), as shown by light microscopy and SEM for barley (Hayward and Parry, 1973) and wheat (Hodson and Sangster, 1988b; 1989b).

Figure 4 illustrates the tissues from a fracture surface of the uppermost (flag) culm leaf from the EO harvest. Microanalyses of frozen leaf fractures have been discussed previously (Hodson and Sangster, 1988a). In the following section these will be compared with analyses of wheat leaves obtained using freeze-substitution and TEM.

Freeze Substitution and TEM

The method of freeze substitution has been widely used in ion localization studies as it permits the retention of soluble components (see Harvey, 1982, 1986 for reviews). The technique involves the rapid freezing of tissue, followed by the substitution

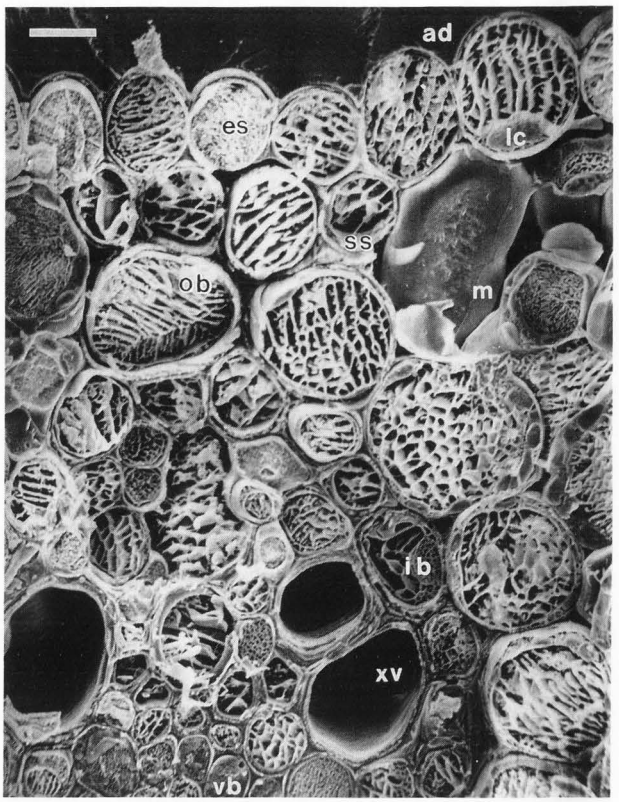

Figure 4. Scanning electron micrograph of a transverse fracture of a bulk-frozen flag leaf blade of T. aestivum at head emergence stage. Ad, adaxial (upper) epidermis; es, epidermal sclerenchyma (above vein); ib, inner bundle sheath; lc, long cell; m, mesophyll; ob, outer bundle sheath; ss, immature subepidermal (costal) sclerenchyma without wall thickening; vb, vascular bundle; xv, xylem vessel. Scale bar = 10 micrometers.

of water within the specimen with a suitable solvent and embedment in resin. Mehard and Volcani (1975) were unable to detect loss of soluble silicon from diatoms when prepared by freeze substitution in ether. Despite these advantages the technique has infrequently been applied to higher plant silicon studies.

Aston and Jones (1976) used freeze substitution to locate soluble monosilicic acid used as a water tracer in the leaves of Avena sterilis. Recently, the technique was applied to the initial stages of mineralization in walls of the lemma macrohairs of the grass Phalaris canariensis which undergo silicification immediately following inflorescence emergence (Hodson and Bell, 1986). They considered that the most probable route for soluble silicon movement within the hair was through the cell wall. K and Cl were the elements that were present at the deposition sites, but this does not imply involvement in the deposition mechanism. Hodson and Sangster (1989c) investigated the wheat root using both cryo-SEM and freeze substitution techniques. Soluble silicon was detected in a series of tissues bridging the root conducting system, suggesting very defined pathways for this element. The following section describes recent data which we obtained using freeze substitution and

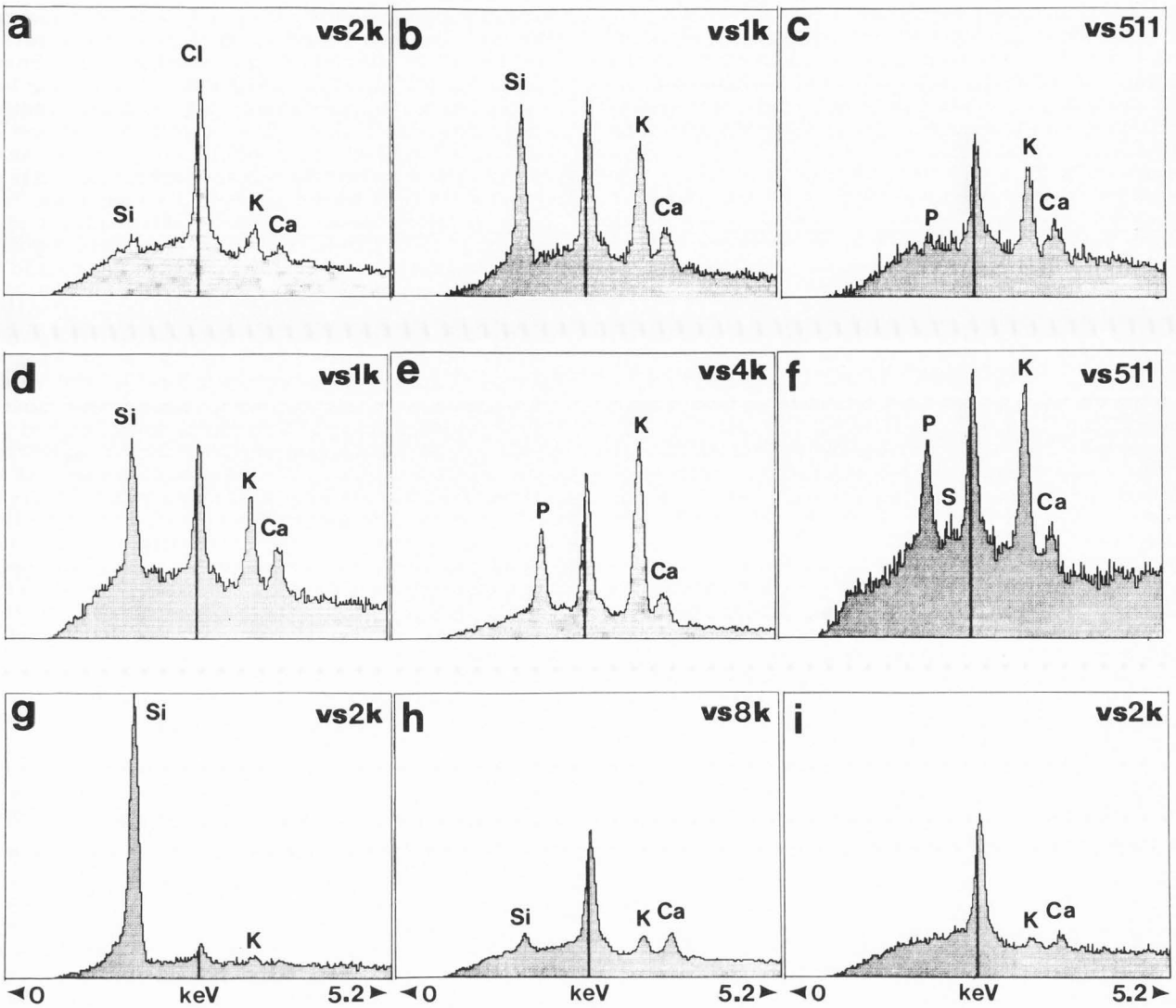

Figure 5. Representative energy dispersive analysis spectra from freeze substituted transverse sections of the blade of basal leaves of wheat grown for 2 weeks in nutrient solution containing 100 ppm SiO_2. Corresponding tissues are illustrated in Fig. 4. Vertical scales (vs) are in counts and horizontal scales in keV. The consistent Cl peak above the central cursor results from resin contamination. **a-d**: adaxial (upper) epidermis; **g-i**: abaxial (lower) epidermis; **a**: intercostal long cell, outer tangential wall (OTW); **b**: sclerenchyma cell (vein), OTW; **c**: sclerenchyma cell protoplasm; **d**: subepidermal sclerenchyma (vein), OTW; **e**: inner bundle sheath cell, protoplasm; **f**: xylem vessel, lumen; **g**: subepidermal sclerenchyma (vein), OTW; **h**: intercostal long cell, OTW; **i**: long cell, protoplasm.

EDX to investigate the wheat leaf.

Plant culture and sample preparation

Triticum aestivum L. cv. Wheaton plants were grown in nutrient solution and segments of fully expanded blades of basal leaves were excised, and prepared by freeze substitution (Mehard and Volcani, 1975; Hodson and Bell, 1986). Leaf segments (1 mm square) were quench-frozen in stirred supercooled propane (-186°C), which was cooled by liquid nitrogen. Frozen samples were transferred to tubes containing ether (dried using molecular sieve type 4A) in a deep freeze at -80°C. Water in the specimens was substituted with ether over 14 days, with three changes of dried ether. Samples were then transferred to anhydrous vinylcyclohexene dioxide (ERL): ether (50:50) at -80°C. Sealed samples were gradually warmed to room temperature over 2 hours and then transferred to anhydrous ERL (100%) in a dry box. Operations at room temperature were conducted in a dry box containing anhydrous calcium chloride, and all solvents and resin components were previously dried over molecular sieve. After two days the samples were taken through an ERL/Spurr resin series, the accelerator being omitted until the 100% resin stage. The resin was polymerized at 60°C for 48 hours. Dry sections (0.5 micrometers) of freeze substituted leaves were cut with glass knives using a Porter Blum Sorval MT2 microtome, and mounted in hinged copper grids (100/100 mesh). Wet sections were also cut and stained for photomicrography (Fig. 1) as previously described.

Analytical electron microscopy

Specimens were examined without carbon coating in a Philips 430 transmission electron microscope fitted with a LINK (10000 AN) energy-dispersive x-ray analyser. For analyses conducted in the transmission mode the operating voltage was 250 kV (LaB_6 filament), the takeoff angle was 15°, the beam current was 2 uamps and the spot size was 70 nm. The counting time for all samples was 100 seconds. Analytical results are presented as x-ray spectra with 0-5.2 keV horizontal scales and variable vertical scales (VS) in counts. Alternatively windows of 0.16 keV were centred around the peaks, and counts were made for 100 seconds. Background radiation was estimated by setting a window of 0.16 keV around an area of the spectrum where there were no peaks (4.50 keV). Blank resin was also analyzed to check for contamination. At least 4 replicate analyses of each tissue area were performed. Results are expressed as peak/background ratios and tested by analysis of variance. It was necessary to remove the counts due to the potassium (K_{beta}) peak from the calcium (K_{alpha}) counts. This was achieved by the analysis of a pure KCl crystal. It was shown that the counts due to potassium (K_{beta}), and which fell within the calcium (K_{alpha}) window, constituted 6.9% of the potassium (K_{alpha}) counts. It was therefore possible to adjust the calcium results, and corrected peak/background ratios are presented here.

In the basal leaf, silicon is present in the sclerenchyma walls of the veins for both epidermi (Figs. 5b, d, g) but not the protoplast (Fig. 5c). While silicon is not entirely absent from the intercostal long cell walls (Figs. 5a, h), which exhibit small peaks, it was not detected in protoplasts (Fig. 5i). Silicon was not detected in the bundle sheath or xylem (Figs. 5e, 5f). Abaxial cells frequently exhibited higher silicon peaks (Fig. 5g) than adaxial cells (Fig. 5d); however, because of wide variability and deposit localization, differences were not significant in Table 1. Conversely, Ca levels were significantly higher (p less than or equal to 0.05) in protoplasts of the adaxial compared to the abaxial epidermal cells. This latter result is not clearly evident in Fig. 5 which includes only two examples (Figs. 5c, i).

Comparisons of specific spectra obtained from freeze substituted sections (Figs. 5a, c, e, f, h, i) with their counterparts obtained from bulk frozen hydrated sections in the previous cryo SEM study of basal wheat leaves (Hodson and Sangster, 1988a) indicates a generally close agreement as regards to the elemental peaks obtained. Additional freeze substitution spectra for the protoplasts of adaxial bulliform and long cells (not shown) also illustrate close agreement in showing consistent Ca peaks compared to virtually no silicon.

Both techniques were applied to the same tissue types; however, it was not possible to compare identical cells. Although we have not attempted quantitative comparisons, the cryo SEM spectra are qualitatively similar to those obtained using freeze substitution, and thus we conclude that the analysis of bulk frozen sections provides a reasonably reliable indication of the elemental species present. However, the potential for error arising from specimen surface geometry or the detectors during this analytical technique must also be recognized (Hodson and Sangster, 1988a).

This latter approach is illustrated by the peak/background ratios of Si, P, K and Ca for representative leaf tissues in Table 1. Because of the mineralized nature of some of the cell walls and the consequent changes in matrix properties when moving between adjacent analysis points, only semi-quantitative comparisons are valid. The results for Ca are of particular interest, being significantly above background (blank resin) in the outer (epidermal) cells as compared to the interior mesophyll tissue of the leaf tissue locations shown on Fig. 4. Although not significantly different in walls, Ca levels are significantly higher in vacuoles of the adaxial compared to the abaxial epidermis (p less than or equal to 0.05). This corroborates a previous comparison of wheat leaf epidermi using cryo-SEM (Hodson and Sangster, 1988a). The epidermal cells appear to be sites of high Ca accumulation in cereal leaves: Gielink et al. (1966), using microautoradiography and freeze substitution observed this phenomenon in oats; Leigh et al. (1986) found high levels of Ca in barley epidermal cells using cryo SEM. The inner bundle sheath is an interior tissue containing above background levels of Ca, P and K. Figure 5e is a spectrum for this tissue. The Si ratios in Table 1 are above background for both the long cell and sclerenchyma walls; however, differences between the surfaces are not significant because of variability. Spectra for leaf tissues, similar to some of those represented in Table 1, include Figs. 5a, d, e, and g to i.

Particle Induced X-ray Emission and Electron Spectroscopic Imaging

Particle induced x-ray emission (PIXE) and its uses is biology are reviewed by Malmqvist (1986) and Maenhaut (1988). In PIXE protons or heavier particles from an electrostatic accelerator are used to induce the emission of characteristic x-rays. The principal advantage of PIXE over electron probe microanalysis is its greater analytical sensitivity, due to a much lower Bremsstrahlung. This greater sensitivity makes it ideal for work on trace elements in biological systems. Soluble silicon levels in most higher plant tissues are at the limits of detection for electron probe microanalysis. PIXE may eventually assist in the localization of soluble silicon. Only two publications have appeared using PIXE to study silicon in higher plant tissues. Perry et al. (1984b) investigated the lemma macrohairs of the grass Phalaris canariensis. In the immature hairs K, P, S and Cl were the dominant elements, while silicon was the dominant element in the mature hairs. Similarly, Hughes et al. (1988) used PIXE to study the stinging emergences of the nettle leaf. Silicon was highest at the emergence tip, while Ca was accumulated in the base of immature emergences. Other elements detected were K, P, S and Mn. In both studies the specimens used were essentially pulled off the living plant, and dried in air or under vacuum. These procedures might have produced some artefactual data, particularly for soluble, highly mobile elements. The major limiting factor in the use of PIXE for biological work is, however, its relatively low spatial resolution. At present the best systems have a minimum beam diameter of about 1 micrometer (Malmqvist, 1986), while beam diameters for electron probe microanalysis in TEM can be as low as 50 nm.

Electron energy loss spectroscopy (EELS) has yet to be applied to higher plant silicon studies.

Table 1. Results of microanalysis of freeze substituted wheat leaves presented as peak/background ratios (mean ± standard deviation for at least 4 analyses)

Cell type	Area analysed	Silicon	Phosphorus	Potassium	Calcium*
Blank resin	---	1.9 ± 0.4	1.8 ± 0.3	1.4 ± 0.1	1.2 ± 0.0
Intercostal adaxial epidermal bulliform	Outer tangential wall	2.7 ± 1.5	2.2 ± 0.6	6.5 ± 4.7	2.8 ± 1.1
	Vacuole	1.6 ± 0.3	1.6 ± 0.3	6.3 ± 5.9	1.5 ± 0.4
Intercostal adaxial epidermal long cell	Outer tangential wall	2.4 ± 0.6	1.7 ± 0.3	9.2 ± 6.7	2.9 ± 1.1
	Vacuole	1.8 ± 0.3	1.2 ± 0.2	6.3 ± 3.0	2.0 ± 0.6
Costal adaxial epidermal long cell	Outer tangential wall	5.7 ± 4.6	1.4 ± 0.5	3.1 ± 1.2	1.9 ± 0.4
	Vacuole	1.5 ± 0.2	1.9 ± 0.5	3.5 ± 0.2	2.5 ± 0.2
Adaxial subepidermal sclerenchyma	Wall	3.2 ± 2.2	1.6 ± 0.2	2.6 ± 0.2	1.7 ± 0.3
	Vacuole	1.4 ± 0.2	1.4 ± 0.1	1.7 ± 0.2	1.3 ± 0.0
Mesophyll	Wall	2.0 ± 0.3	3.4 ± 1.4	6.2 ± 1.8	1.3 ± 0.2
	Vacuole	2.0 ± 0.2	3.9 ± 1.5	8.4 ± 3.5	1.2 ± 0.2
Metaxylem vessel	Wall	1.3 ± 0.2	1.6 ± 0.3	2.5 ± 0.9	1.4 ± 0.1
	Lumen	1.3 ± 0.1	1.8 ± 0.7	2.2 ± 0.8	1.4 ± 0.1
Inner bundle sheath	Wall	1.7 ± 0.2	2.4 ± 0.8	4.2 ± 1.6	2.3 ± 0.5
	Vacuole	1.8 ± 0.3	4.3 ± 2.4	6.6 ± 4.5	1.9 ± 0.3
Outer bundle sheath	Wall	1.4 ± 0.4	1.5 ± 0.2	2.4 ± 0.9	1.5 ± 0.2
	Vacuole	1.3 ± 0.6	1.6 ± 0.4	3.1 ± 1.3	1.4 ± 0.2
Abaxial subepidermal sclerenchyma	Wall	4.5 ± 6.5	1.0 ± 0.4	1.4 ± 0.4	1.2 ± 0.3
	Vacuole	1.0 ± 0.3	1.1 ± 0.3	1.2 ± 0.3	1.1 ± 0.2
Costal abaxial epidermal long cell	Outer tangential wall	4.7 ± 3.6	1.5 ± 0.2	3.2 ± 1.5	2.0 ± 0.5
	Vacuole	1.5 ± 0.6	1.5 ± 0.4	2.5 ± 1.2	1.7 ± 0.6
Intercostal abaxial epidermal long cell	Outer tangential wall	3.9 ± 2.7	1.6 ± 0.2	3.6 ± 1.9	2.2 ± 0.8
	Vacuole	1.5 ± 0.3	1.5 ± 0.2	3.0 ± 2.7	1.5 ± 0.3

*values corrected to remove counts due to potassium (K_{beta}).

EELS has a spatial resolution of only 0.5 nm and is considerably more sensitive than EDX (Ottensmeyer and Andrew, 1980). Using this technology, Rogerson et al. (1987) reported soluble silicon in the cytoplasm in the diatom Thalassiosira pseudonana, in ribosomes and lipid inclusions. Unfortunately, Rogerson et al. used conventional preparatory techniques prior to analysis, which can lead to considerable loss and redistribution of silicon. At present EELS requires ultrathin sections of only 30 nm in thickness. This may be a serious limitation as such sections can only realistically be cut on to water, and loss of soluble components at this stage would appear to be inevitable.

Conclusions

When investigating deposited, immobile silica in higher plants conventional preparatory techniques are usually adequate and EDX is easily able to detect deposited silica. Attention has, however, been switching to studies of soluble silicon, and of the ionic environment at deposition sites. Two major techniques have emerged to facilitate these studies: EDX analysis on the cold stage of an SEM and analysis of freeze substituted sections in TEM or scanning transmission electron microscope. The usefulness of these two techniques is limited to some extent by the lack of analytical sensitivity of EDX, and soluble silicon can at present only be reliably located in tissues where it seems to be concentrated to a considerable extent (e.g., lemma macrohairs: Hodson and Bell, 1986; wheat root metaxylem: Hodson and Sangster, 1989c). In the future it is possible that PIXE and/or EELS will be developed to assist in our investigations of higher plant silicon.

Acknowledgements

The authors are indebted to the following individuals who made significant contributions to this study: Mr. D. Holmyard [electron microscope facility, connective tissue research group (Head, Dr. K.P.H. Pritzker)], Mount Sinai Hospital, Toronto; Ms. J.

Carson (Biology Dept., McMaster University, Hamilton, Ontario, who supervised the SEM and cryostageanalyses); Prof. I.B. Heath and Mrs. S.G.W. Kaminskyj (Department of Biology, York University for providing the propane freezing facility); The School of Animal Biology, University College of North Wales, Bangor, U.K. (for making their TEM facilities available, and Mrs. A.V. Buckland assisted with the sectioning); Mr. J. Dawson (DIAR, York University who produced the photographic plates). The study was financed by a grant from the Natural Sciences and Engineering Research Council (Canada).

References

Aston MJ, Jones MM (1976) A study of the transpiration surfaces of Avena sterilis L. var. Algerian leaves using monosilicic acid as a tracer for water movement. Planta 130, 121-129.

Bennett DM, Sangster AG (1982) Electron-probe microanalysis of silicon in the adventitious roots and terminal internode of the culm of Zea mays. Can. J. Bot. 60, 2024-2031.

Dayanandan P (1983) Localization of silica and calcium carbonate in plants. Scanning Electron Microsc. 1983; III: 1519-1524.

Dayanandan P, Hebard FV, Kaufman PB (1976) Cell elongation in the grass pulvinus in response to geotropic stimulation and auxin application. Planta 131, 245-252.

Dayanandan P, Kaufman PB (1976) Trichomes of Cannabis sativa L. (Cannabaceae). Amer. J. Bot 63 578-591.

Dinsdale D, Gordon AH, George S (1979) Silica in the mesophyll cell walls of Italian rye grass Lolium multiflorum Lam. cv. RvP. Ann. Bot. 44, 73-77.

Djamin A, Pathak MD (1967) Role of silica in resistance to Asiatic rice borer, Chilo suppressalis (Walker) in rice varieties. J. Econ. Ent. 60, 347-351.

Eleuterius LN, Lanning DC (1987) Silica in relation to leaf decomposition of Juncus roemerianus. J. Coastal Res. 3, 531-534.

Eschrich W, Fromm J, Essiamah S (1988) Mineral partitioning in the phloem during autumn senescence of beech leaves. Trees 2, 73-83.

Fritz E (1989) X-ray microanalysis of diffusible elements in plant cells after freeze-drying, pressure-infiltration with ether and embedding in plastic. Scanning Microsc. 3, 517-526.

Gartner S, Le Faucheur L, Roinel N, Paris-Pireyre N (1984) Preliminary studies on the elemental composition of xylem exudate from two varieties of wheat by electron probe analysis. Scanning Electron Microsc. 1984; IV: 1739-1744.

Gartner S, Paris-Pireyre N (1984) La silice chez le ble (Triticum aestivum L.). Comparaison entre une variete sensible et une variete resistante a la verse (Silica in wheat (Triticum aestivum L.). Comparison between a susceptible variety and a variety resistant to lodging). J. Phys. (Paris) Colloque C2, 45, 511-514.

Gielink AJ, Sauer G, Ringoet A (1966) Histo-autoradiographic localization of calcium in oat plant tissues. Stain Technol. 41, 281-286.

Hansen DJ, Dayanandan P, Kaufman PB, Brotherson JD (1976) Ecological adaptations of salt marsh grass, Distichlis spicata. (Gramineae), and environmental factors affecting its growth and distribution. Amer. J. Bot. 63, 635-650.

Harvey DMR (1982) Freeze-substitution. J. Microsc. 127, 209-221.

Harvey DMR (1986) Applications of x-ray microanalysis in botanical research. Scanning Electron Microsc. 1986; III: 953-973.

Hayward DM, Parry DW (1973) Electron-probe microanalysis studies of silica distribution in barley (Hordeum sativum L.). Ann. Bot. 37, 579-591.

Heath MC (1981) Insoluble silicon in necrotic cowpea cells following infection with an incompatible isolate of the cowpea rust fungus. Physiol. Plant Pathol. 19, 273-276.

Hodson MJ, Bell A (1986) The mineral relations of the lemma of Phalaris canariensis L., with particular reference to its silicified macrohairs. Israel J. Bot. 35, 241-253.

Hodson MJ, Sangster AG (1988a) Observations on the distribution of mineral elements in the leaf of wheat (Triticum aestivum L.) with particular reference to silicon. Ann. Bot. 62, 463-471.

Hodson MJ, Sangster AG (1988b) Silica deposition in the inflorescence bracts of wheat (Triticum aestivum L.). I. Scanning electron microscopy and light microscopy. Can. J. Bot. 66, 829-838.

Hodson MJ, Sangster AG (1989a) X-ray microanalysis of the seminal root of Sorghum bicolor (L.) Moench. with particular reference to silicon. Ann. Bot. 64, 659-667.

Hodson MJ, Sangster AG (1989b) Silica deposition in the inflorescence bracts of wheat (Triticum aestivum L.) II. X-ray microanalysis and backscattered electron imaging. Can. J. Bot. 67, 281-287.

Hodson MJ, Sangster AG (1989c) Subcellular localization of mineral deposits in the roots of wheat (Triticum aestivum L.) Protoplasma 151, 19-32.

Hodson MJ, Sangster AG, Parry DW (1984) An ultrastructural study on the development of silicified tissues in the lemma of Phalaris canariensis L. Proc. Royal Soc. Lond. B 222, 413-425.

Hodson MJ, Sangster AG, Parry DW (1985) An ultrastructural study on the developmental phases and silicification of the glumes of Phalaris canariensis L. Ann. Bot. 55, 649-665.

Hughes NP, Perry CC, Williams RJP, Watt F, Grime GW (1988) A scanning proton microprobe study of stinging emergences from the leaf of the common stinging nettle Urtica dioica L. Nucl. Instrum. Methods Phys. Res. Sect. B 30, 383-387.

Iler RK (1955) The Colloid Chemistry of Silica and Silicates, Cornell Univ. Press, Ithaca, NY, pp. 18-31.

Kaufman PB, Bigelow WC, Petering LB, Drogosz FB (1969) Silica in developing epidermal cells of Avena internodes: Electron microprobe analysis. Science 166, 1015-1017.

Kaufman PB, Petering LB, Smith JG (1970) Ultrastructural development of cork-silica cell pairs in Avena internodal epidermis. Bot. Gaz. 131, 173-185.

Kaufman PB, Dayanandan P, Takeoka Y, Bigelow WC, Jones JD, Iler RK (1981) Silica in shoots of higher plants. In: Silicon and Siliceous Structures in Biological Systems. Simpson TL, Volcani BE (eds.), Springer-Verlag, New York, pp 409-449.

Laroche J (1967) Localisation de la silice par le microanalyseur a sonde electronique (Detection of silicon by the electron-probe microanalyzer). Compt. Rend. Acad. Sci. (Paris) 265, 1695-1697.

Lauchli A, Schwander H (1966) X-ray microanalyser study on the location of minerals in native

plant tissue sections. Experientia 22, 503-505.

Leigh RA, Chater M, Storey R, Johnston AE (1986) Accumulation and subcellular distribution of cations in relation to the growth of potassium-deficient barley. Plant, Cell and Environ. 9, 595-604.

Maenhaut W (1988) Applications of ion beam analysis in biology and medicine, a review. Nucl. Instrum. Methods Phys. Res. Sect. B 35, 388-403.

Malmqvist KG (1986) Proton microprobe analysis in biology. Scanning Electron Microsc. 1986; III: 821-845.

Mehard CW, Volcani BE (1975) Evaluation of silicon and germanium retention in rat tissues and diatoms during cell and organelle preparation for electron probe microanalysis. J. Histochem. Cytochem. 23, 348-358.

Metcalfe CR (1960) Anatomy of the Monocotyledons. I. Gramineae. Oxford, London, pp. 656-713.

Montgomery DJ, Parry DW (1979) The ultrastructure and analytical microscopy of silicon deposition in the intercellular spaces of the roots of Molinia caerulea (L.) Moench. Ann. Bot 44, 79-84.

Ollendorf AL (1987) Archaeological implications of a phytolith study at Tel Miqne (Ekron), Israel. J. Field Archaeol. 14, 453-463.

Ottensmeyer FP, Andrew JW (1980) High resolution microanalysis of biological specimens by electron energy loss spectroscopy and by electron spectroscopic imaging. J. Ultrastruct. Res. 72, 336-348.

Parry DW, Hodson MJ, Sangster AG (1984) Some recent advances in studies of silicon in higher plants. Phil. Trans. Royal Soc. Lond. B. 304, 537-549.

Parry DW, Kelso M (1977) The ultrastructure and analytical microscopy of silicon deposits in the roots of Saccharum officinarum (L.). Ann. Bot. 41, 855-862.

Perry CC, Mann S, Williams RJP (1984a) Structural and analytical studies of the silicified macrohairs from the lemma of the grass Phalaris canariensis L. Proc. R. Soc. Lond. B 222, 427-438.

Perry CC, Mann S, Williams RJP, Watt F, Grime GW, Takacs J (1984b) A scanning proton microprobe study of macrohairs from the lemma of the grass Phalaris canariensis L. Proc. Royal Soc. Lond. B. 222 439-445.

Piperno DR (1988) Phytolith Analysis. An Archaeological and Geological Perspective. Academic Press, London, pp. 50-198.

Raven JA (1983) The transport and function of silicon in plants. Biol. Rev. 58, 179-207.

Reynolds ES (1963) The use of lead citrate at high pH as an electron-opaque stain in electron microscopy. J. Cell Biol. 17, 208-212.

Rogerson A, De Freitas ASW, McInnes AG (1987) Cytoplasmic silicon in the centric diatom Thalassiosira pseudonana localized by electron spectroscopic imaging. Can. J. Microbiol. 33, 128-131.

Sakai WS, Thom M (1979) Localisation of silicon in specific cell wall layers of the stomatal apparatus of sugar cane by use of energy dispersive x-ray analysis. Ann. Bot. 44 245-248.

Sangster AG, Hodson MJ (1986) Silica in higher plants. In: Silicon Biochemistry, CIBA Foundation Symposium 121, Wiley, Chichester, U.K., pp. 90-111.

Sangster AG, Parry DW (1976) The ultrastructure and electron-probe microassay of silicon deposits in the endodermis of the seminal roots of Sorghum bicolor (L.) Moench. Ann. Bot. 40, 447-459.

Sangster AG, Parry DW (1981) Ultrastructure of silica deposits in higher plants. In: Silicon and Siliceous Structures in Biological Systems. Simpson TL, Volcani BE (eds.), Springer-Verlag, New York, pp. 383-407.

Sangster AG, Hodson MJ, Parry DW, Rees JA (1983) A developmental study of silicification in the trichomes and associated epidermal structures of the inflorescence bracts of the grass Phalaris canariensis L. Ann. Bot. 52, 171-187.

Werner D, Roth R (1983) Silica metabolism. Encyclopedia of Plant Physiology New Series Volume 15B. Lauchli A, Beileski RL (eds.), Springer-Verlag, Berlin, pp. 682-694.

Discussion with Reviewers

H.F. Mayland: The authors have demonstrated that sample preparation is important in obtaining true images for microanalysis. The assumption that silicon is passively absorbed is now questioned by results of this and other studies like that of S.C. Jarvis, Plant and Soil 97:429-437 (1987). Are there other hypotheses about elemental uptake and distribution that may be challenged when using techniques that reduce leaching of nutrients?

Authors: X-ray microanalysis has already increased our understanding of many areas in higher plant physiology. We would cite the considerable influence microanalytical work has had in the field of salt tolerance. As a by-product of our own work we have found that the shoot epidermal cells in grasses and cereals seem to accumulate high levels of soluble calcium and/or chloride: a totally unexpected result.

S.D. Russell: Presumably, Si accumulated from the substrate enters the plant and undergoes long distance translocation within the xylem, as suggested here and elsewhere. This presumably places most of the soluble Si into the apoplast. Can you make any conclusions about whether significant amounts of soluble silicon enter the symplast, and if so, which subcellular compartments appear to be involved?

Authors: The data available at present suggests that silicon is largely, but not completely, excluded from the symplast in most plant cell types. (At least until phytolith formation occurs in the cell lumen). We have detected low levels of symplastic silicon in many cells from both shoot and root, but are hampered at present by the lack of sensitivity of the available detection systems. As yet we have little data at the subcellular level, but the vacuole may be important in this respect (Hodson & Bell, 1986).

S.D. Russell: In the light of the wide area of the probe in the SEM, and particularly in view of the relatively massive ice crystal damage occurring during cryo-SEM, what assurance do you have that concentration of solutes measured in point analyses are not increased by their separation in the forming eutectic?

Authors: Ice crystal formation is undoubtedly a problem in cryo-SEM, and increased concentrations of solutes are a possibility. This will be an even greater problem for wholly quantitative work. We suggest that many analyses are conducted, and that the results are compared with those from other techniques (e.g., conventional mineral analysis and freeze substitution followed by EDX in TEM).

G.M. Roomans: It is well-known that contamination of samples with Si easily occurs. How do you prevent or take this contamination into account?
Authors: Both microscopes we used were fitted with anti-contamination cold fingers. As an additional precaution we were careful to analyse blank resin (Table 1) to compare with tissue analyses. Blank resin levels were consistently much lower than those from mineralized areas.

G.M. Roomans: Why did you use an accelerating voltage of 250 kV for the analysis of the freeze-substituted material? Was this necessary to get an image? Could you show an image of the specimen?
Authors: The 250 kV accelerating voltage gave us a much better image, and only slightly reduced the sensitivity of our analyses. The images of dry-cut, unstained, thick sections of plant material are rather poor. We prefer to cut thin sections on to water after we have cut the dry sections for analysis. These can then be stained, and ultrastructural details can be observed (Fig. 1 is an example of the thin section from a wheat leaf prepared in this way).

E. Fritz: How reliable is the localization of the electron beam in the protoplasm? Figs. 2a and 4 show a rather deep etching, therefore an electron beam of 15 kV would penetrate rather deeply into the dry tissue and may not be restricted only to the protoplasm.
Authors: This is indeed a problem with this technique. We did attempt analyses of material that was not etched, but cellular detail was obscured, and it was difficult to be sure what was being analysed. Where possible we have followed cryo-SEM with freeze substitution and analysis in TEM. Thus far the results from the two techniques have been comparable, at least on a semi quantitative basis.

E. Fritz: Table 1 shows unusual high contents of P, K and Ca in blank resin. To my experience, a K peak to background ratio of 1.36 (Table 1) would correspond to about 30 mmolar K in the resin. How can this be explained? Microanalytical results in our laboratory with freeze-dried plant tissue which was embedded in Spurr's resin did not show any P, K and Ca peaks in blank resin (Fromm, personal communication).
Authors: Biomineralized material presents some technical difficulties for qualitative work. Where deposition occurs the silicon peak is often so large that it increases the background radiation in the adjacent areas of the spectrum. It is thus not possible to use peak to background ratios derived from peaks and the computed background beneath them. We use instead total counts under the elemental peak over the background counts estimated by setting a window of 0.16 keV in an area of the spectrum with no peaks (4.50 keV). This has the effect that our peak to background ratios increase where the Bremsstrahlung radiation is highest. Our peak to background ratios are thus not directly comparable with those of Dr. Fritz. Therefore the spectra obtained from blank Spurr's resin in our work also do not show P, K and Ca peaks. We included the blank resin results to compare with the tissue analyses.

E. Fritz: What was the reason for setting such a narrow window of 0.16 keV to measure the background radiation? Counting statistics would be better in a broader window as is usually done.
Authors: The 0.16 keV window was used as it was directly comparable with the windows used for elemental analyses, and this was required for our method of calculating peak to background ratios.

E. Fritz: Is it possible to derive from the Si content of the tissue some evidence for the pathway of Si movement in the tissue? Si may be accumulated at sites different from the pathway.
Authors: Of course, it is not possible to derive definite pathways for silicon movement from our x-ray microanalytical data, in which silicon distribution is assessed at a single instant in time. In the aerial parts of many grasses and cereals silica, which is mostly transported in the xylem, is mainly deposited in the epidermal cells. It is therefore possible to postulate pathways between the xylem and the epidermis, although the proof that these are functional is still required.